Tissue growth associated transition of podoplanin-expressing stromal cells in the postnatal mouse femur

Hinako Notoh[a], Rikuto Nara[a], Nobuaki Suzuki[b], Atsuo Suzuki[c], Shuichi Okamoto[d], Nagaharu Tsukiji[e], Takeshi Kanematsu[f], Naruko Suzuki[f], Akira Katsumi[g], Tetsuhito Kojima[d,h], Katsue Suzuki-Inoue[e], Tadashi Matsushita[b,f], Shogo Tamura[b,i,*]

[a]Graduate School of Health Sciences, Hokkaido University, Japan

[b]Department of Transfusion Medicine, Nagoya University Hospital, Nagoya, Japan

[c]Department of Medical Technique, Nagoya University Hospital, Nagoya, Japan

[d]Department of Integrated Health Sciences, Nagoya University Graduate School of Medicine, Nagoya, Japan

[e]Department of Clinical and Laboratory Medicine, Faculty of Medicine, University of Yamanashi, Chuo, Yamanashi, Japan

[f]Department of Clinical Laboratory, Nagoya University Hospital, Nagoya, Japan

[g]Department of Hematology, National Center for Geriatrics and Gerontology, Obu City, Japan

[h]Aichi Health Promotion Foundation, Nagoya, Japan

[i]Department of Clinical Laboratory Science, Faculty of Health Sciences, Hokkaido University, Sapporo, Japan

* Corresponding author

Shogo Tamura, Ph.D.

Department of Clinical Laboratory Science, Faculty of Health Sciences, Hokkaido University,

Kita-12 Nishi-5, Kita-Ku, Sapporo 060-0812, Japan

Tel/Fax: +81 11 706 3384, E-mail: stamura@hs.hokudai.ac.jp

Running Headline/Short Title

PDPN-stromal cells in the neonatal femur

Abstract

Skeletal stem/progenitor cells are tissue-resident stem/progenitor cells involved in the formation of the skeletal tissue, bone marrow, and hematopoietic microenvironment**.** Podoplanin-expressing stromal cells (PDPN-SCs) are skeletal stem/progenitor cell-lineage stromal cells. In the adult mouse bone marrow, PDPN-SCs are present on the diaphyseal arterioles and promote megakaryo/erythropoiesis. However, the localized distribution of PDPN-SCs in neonatal and postnatal femurs remains unclear. In this study, we histologically examined the transition of PDPN-SCs during postnatal femoral growth. In the diaphyseal marrow, PDPN-SCs were present in the neonatal marrow space but disappeared with femoral growth. In the cortical bone, abundant PDPN-SCs existed in the primitive neonatal bone and transitioned to restricted localization in the periosteum and endosteum with tissue growth. In the metaphysis, PDPN-SCs resided in nascent trabecular bones. We also found a novel subset of PDPN-SCs that expressed osterix, suggesting that osterix-positive PDPN-SCs were involved in bone formation. Furthermore, in the diaphyseal arterioles, periarteriolar PDPN-SCs appeared sporadically between 1–2 weeks of age and populated to surround the arterioles. These histological observations can contribute to the understanding of how stromal cells, including PDPN-SCs, engage in postnatal bone and marrow formation.

Keywords: Podoplanin, stromal cell, bone, bone marrow.

Introduction

Bone and bone marrow formation occurs in two distinct fetal/neonatal development processes called intramembranous and endochondral ossification [1]. Intramembranous ossification is the developmental process of flat bones such as the skull and clavicle. In this process, the bone is directly differentiated from the mesenchymal stem/stromal cells in the soft connective tissue. Endochondral ossification is a process of bone and marrow development that forms all bones of the body except for flat bones. In endochondral ossification, bone and marrow development is initiated from the avascular primitive cartilage. Perichondral vasculatures, mesenchymal stem/stromal cells, and skeletal cells such as bone-forming osteoblasts and resorbing osteoclasts/chondroclasts invade and populate the cartilage [2-4]. In long bones, such as the femur, the invading vasculature, and skeletal cells generate a marrow cavity within the cartilage, which is transformed into a fetal primary ossification center (POC) in the middle part of the diaphysis and a neonatal secondary ossification center (SOC) in the epiphysis [5]. In the POC-related portions of the femur, trabecular bones are formed at the longitudinal ends of the marrow cavity, and cortical bones surround the peripheral zone of the diaphysis.

Mesenchymal stem cells (MSCs) or mesenchymal stem/progenitor cells (MSPCs) are tissue-resident somatic stem cells that can self-renew and undergo multilineage differentiation, particularly mesenchymal trilineage differentiation, including osteogenesis, adipogenesis, and

chondrogenesis [6]. MSCs and their progeny can be isolated from various tissues, such as the umbilical cord, adipose tissue, and bone marrow, in humans and mice. Recently, MSCs in the bone marrow [7-18], periosteum [19-22], and growth plate resting zone [23, 24] have been renamed skeletal stem/progenitor cells (SSCs) because they are functionally specialized for the development, homeostasis, and regeneration of the skeletal system and the hematopoietic microenvironment in the bone marrow [25].

Podoplanin (PDPN, also known as gp38 or T1a)-expressing stromal cells (PDPN-SCs) are SSC progeny with regulatory functions in vascular integrity and hematopoiesis in the bone marrow [26-28]. In the epiphysis, periosteal PDPN-SCs invade the nascent epiphyseal marrow and regulate the integrity of the primitive vasculature network during postnatal SOC formation [26]. In adult mice (>8 weeks old), PDPN-SCs reside in the marrow arterioles and generate a megakaryo/erythropoiesis-promoting microenvironment in the periarteriolar region of the diaphyseal marrow [27, 29]. PDPN-SCs are also present in the periosteum of adult diaphyseal cortical bones [28]. However, the biological machinery through which PDPN-SCs populate the marrow, periosteum, and other POC-related portions of the femur has not yet been elucidated.

This study aimed to investigate the tissue growth-associated spatiotemporal distribution and transition of PDPN-SCs in the femur, especially in POC-related femoral regions, diaphyseal marrow, cortical bone, and metaphysis. The findings of this study will provide new insights

into the involvement of stromal cells, including PDPN-SCs, in bone/marrow development and growth.

Materials and Methods

Mice

The C57BL/6NJc1 mice were purchased from CLEA Japan (Tokyo, Japan). Mice were bred and maintained under standard conditions [12 h light/dark cycle with stable temperature (25 °C) and humidity (60%)]. This study was approved by the Animal Care and Use Committee of the Hokkaido University (22-0087).

Preparation of tissue sections

Femurs were fixed with 4% paraformaldehyde (PFA, Wako) for 24 h and subsequently decalcified for 16 h for 3–5 days (depending on the age of the mice) using K-CX (FALMA). After washing with diluted water, the bone pieces were incubated with 30% sucrose in phosphate-buffered saline (PBS) for cryoprotection and 15% sucrose diluted with Tissue-Tek O.C.T. Compound (Tissue-Tek). Treated tissues were embedded in Tissue-Tek O.C.T. Compound at −80 °C. Frozen sections were sectioned at a thickness of 20-μm by cryostat (Leika CM1950).

Immunohistochemical staining

The frozen sections were blocked using Blocking One Histo (Nacalai Tesque) for 7 min and washed with 0.05% phosphate-buffered saline-Tween 20 (PBS-T) for 10 min. Fc blocking

was performed using rat anti-mouse CD16/CD32 (BD Biosciences, 1:200 dilution with antibody diluent) for 30 min. The antibody diluent was a diluted-Blocking One Histo (1:20 dilution in PBS-T). After washing twice with PBS-T for 10 min, the sections were probed using primary antibodies overnight at 4 °C. Sections probed with primary antibodies were washed twice and subsequently incubated with each secondary antibody for 1.5 h. The antibodies used in this study are listed in Supplementary Table S1. In the case of double immunostaining using anti-CD31 goat polyclonal antibody and anti-PDPN hamster monoclonal antibody, we probed sections using a sequential staining procedure, 1st antibody (1st primary antibody): anti-CD31 goat polyclonal antibody, 2nd antibody: anti-goat immunoglobulin donkey IgG fluorescein conjugate, 3rd antibody (2nd primary antibody): anti-PDPN hamster monoclonal antibody, 4th antibody: anti-hamster immunoglobulin goat IgG fluorescein conjugate. Sections were mounted with VECTASHIELD Antifade Mounting Medium containing DAPI (Vector Laboratories) and observed under an upright fluorescence microscope (ECRIPSE E600; Nikon). The acquired images were analyzed using ImageJ 1.46r software (http://rsb.info.nih.gov/ij/).

Quantitative image data analysis (area measurement and cell count)

The number of PDPN-SCs in the cortical bone was counted in short-axis sections (n = 3 each). The number of PDPN-SCs in the diaphyseal marrow and metaphysis was counted in the long-

axis femur sections (n = 3 each). The CD31-positive area within the diaphyseal marrow and cortical bone was measured in the short-axis section of 0–3-week-old mouse femurs (n = 3 each). The CD31-positive area of each femur was calculated as the average of the areas in the proximal, central, and distal portions. The area index, which was calculated using the areas of the metaphysis and diaphysis, was designed to assess the metaphysis growth. The areas of the metaphysis and diaphysis were measured along the long axis of the mouse femurs (n = 3). Data analysis was performed using ImageJ software.

Statistical analysis

Quantitative data are depicted as mean ± SD values of the mean. Multigroup comparisons were performed using one-way analysis of variance (ANOVA) and Tukey's multiple comparison test. Statistical correlations were calculated using Pearson's correlation test. Statistical analyses were performed using GraphPad Prism version 5.

Results

Localized distribution of PDPN-SCs in the postnatal femur

In adult mice, the PDPN-SCs were detected at arterioles of the diaphyseal marrow and periosteum [27, 28]. To investigate the spatiotemporal behavior of PDPN-SCs in the POC-related diaphyseal region of the femur, we first histologically determined the distribution of PDPN-SCs in postnatal mouse femurs (Fig. 1). In this study, postnatal bone and marrow growth was assessed based on their vascular structures. Although there are some differences in their CD31-expression intensity, the blood vessels of the bone marrow widely express CD31. In the femur of adult mice, vasculatures with CD31-high expression in the arterioles and metaphysis are termed H-type vessels, and those with CD31-low expression in the sinusoids are termed L-type vessels [30, 31]. Fig. 1A shows a schematic of the femur. In the femurs of newborns (postnatal day 0, shown as 0 weeks old: 0 w.o), CD31 high-expressing blood vessels were entirely observed in the POC-related primitive diaphyseal marrow, cortical bone, and metaphysis (Fig. 1B–D). PDPN-SCs were detected in the primitive diaphyseal marrow, cortical bone, metaphysis, and also periosteum. In the femur of 1 w.o mice (Fig. 1E–G), trabecular bones were formed in the metaphysis, and the diaphyseal marrow was clearly distinguished in the structures. High CD31 expression was observed in the blood vessels of the diaphyseal marrow, metaphysis, and cortical bones. PDPN-SCs were detected on the metaphyseal trabecular bones and within the cortical bone but not in the diaphyseal marrow.

In 2 w.o mice (Fig. 1H–J), CD31 high-expressing blood vessels were observed in the metaphysis and diaphyseal arterioles. CD31 low-expressing vessels were abundant in the diaphyseal marrow. At this point, the number of vessels in the cortical bone was drastically reduced. PDPN-SCs were mainly detected on the metaphyseal trabecular bones and peri/endosteum of the cortical bone. Several PDPN-SCs were still present in the cortical bone. The diaphyseal arterioles were not ensheathed with PDPN-SCs at 2 w.o (Fig. 1H, inner panel). In 3 w.o mice (Fig. 1K–M), the vascular pattern of the diaphyseal marrow was identical to that of the femur of 2 w.o mice. CD31 high expression was observed in the diaphyseal arterioles and the metaphysis. PDPN-SCs were restrictedly detected in the diaphyseal arterioles and several parts of the peri/endosteum (Fig. 1K, inner panel, and Fig. 1M). These observations indicate that the diaphyseal marrow vascular network develops into a mature pattern at two weeks of age in mice, after which the diaphyseal arterioles are ensheathed by PDPN-SCs. In addition, PDPN-SCs are present within the primitive cortical bone of neonates and are likely to decrease in number with postnatal ontogenetic growth.

PDPN-SCs in the femoral POC-related regions decrease in association with tissue growth

Given the observations of histological screening, we quantitatively evaluated PDPN-SCs in POC-related regions of the femur (Fig. 2). The number of PDPN-SCs in the diaphyseal

marrow, cortical bone, and metaphysis was counted in longitudinal or transverse sections of the femurs. In the diaphyseal marrow (Fig. 2A and B), PDPN-SCs were significantly decreased within one week after birth and subsequently disappeared (number of PDPN-SCs in the diaphyseal marrow: 297.93 ± 76.07 cells in 0 w.o, 51.13 ± 48.43 cells in 1 w.o, and 9.67 ± 5.73 cells in 2 w.o). In the cortical bone, including the periosteum and endosteum (Fig. 2C and D), PDPN-SCs decreased slightly, but not significantly, in the first week of birth and significantly in the following week (number of PDPN-SCs in the cortical bone: 217.147 ± 540.55 cells in 0 w.o, 1328.89 ± 319.55 cells in 1 w.o, and 980.12 ± 267.30 cells in 2 w.o). At 2 w.o, PDPN-SCs in the diaphyseal cortex are restricted to the periosteum and some portions of the endosteum. In the metaphysis (Fig. 2E and F), the number of PDPN-SCs did not change within the first week of birth, whereas a significant decrease in PDPN-SCs was detected in the 2. w.o femurs (number of PDPN-SCs in the metaphysis: 666.22 ± 153.37 cells in 0 w.o, 590.30 ± 75.38 cells in 1 w.o, and 363.31 ± 60.71 cells in 2 w.o). These results indicate that the number and localized distribution of PDPN-SCs in the femur change with the stages of postnatal tissue growth.

To confirm whether the behavior of PDPN-SCs in the bone and marrow is associated with postnatal ontogeny, we assessed the correlation between the number of PDPN-SCs and tissue growth in the diaphyseal marrow, cortical bone, and metaphysis (Fig. 3). The vascular network area (CD31-positive area) was used as an index of tissue growth in the diaphyseal

marrow and cortical bone. In the metaphysis, the area index, which was calculated from the area of the metaphysis and diaphysis, was designed because their vascular network does not seem to change with ontogeny. In the diaphyseal marrow, the CD31-positive area was decreased with the marrow growth (15.93 ± 1.48% in 0 w.o, 7.77 ± 2.97% in 1 w.o, and 6.23 ± 3.44% in 2 w.o, Fig. 3A), and PDPN-SCs and the CD31-positive area within the growing diaphyseal marrow was correlated (R squared = 0.99, $p < 0.05$, Fig. 3B). In the cortical bone, the CD31-positive area was also decreased with the bone growth (9.40 ± 0.98% in 0 w.o, 3.37 ± 1.95% in 1 w.o, and 1.00 ± 0.69% in 2 w.o, Fig. 3C), and PDPN-SCs and the CD31-positive area within the growing cortical bone was correlated (R squared = 1.00, $p < 0.01$, Fig. 3D). These results revealed that the number of PDPN-SCs in the diaphyseal marrow and cortical bone decreases with tissue growth. In the metaphysis, the area index was gradually decreased with femur growth (0.47 ± 0.16% in 0 w.o, 0.26 ± 0.13% in 1 w.o, and 0.11 ± 0.02% in 2 w.o, Fig. 3E). PDPN-SCs and the metaphyseal area index showed a tendency to correlate but were not statistically significant (R squared = 0.89, $p = 0.2191$, Fig. 3F). The approximate curve was shown to be convex downward, suggesting that metaphyseal PDPN-SCs declined in number after tissue growth.

A subset of PDPN-SCs expresses osterix

In the diaphyseal marrow, cortical bone, and metaphysis, PDPN-SCs decrease their

numbers with tissue growth. We previously reported that epiphyseal PDPN-SCs possessed the ability to differentiate into osteoblasts [26]. These insights led to the hypothesis that PDPN-SCs are committed to the tissue portions of the femur, especially the bone parenchyma. To investigate this hypothesis, we examined whether PDPN-SCs expressed osterix (OSX), an osteogenic transcription factor, in pre-osteoblasts [5]. Immunohistochemistry (IHC) analysis revealed that the PDPN-SCs included two subsets: OSX-positive and -negative cells (Fig. 4). In the diaphyseal marrow during 0–1 w.o, OSX-positive signals were detected in a part of PDPN-SCs (Fig. 4A). In the cortical bone, OSX-positive cells were widely detected in the cortex of 0–1 w.o and decreased with age progression (Fig. 4B). The periosteum was OSX-positive throughout the 0–3 w.o mice. The OSX expression pattern of PDPN-SCs within the cortical bone gradually changed with tissue growth. At ages 0 and 1 w.o, most PDPN-SCs were OSX-positive, whereas OSX-negative PDPN-SCs were prominent from two weeks onward. In the metaphysis, age 0 w.o, OSX-positive and -negative PDPN-SCs were detected in the primitive metaphysis (Fig. 4C). Both PDPN-SCs with OSX-positive and -negative cells resided in the peri-trabecular region, and these PDPN-SCs were present throughout the 1–3 w.o. These observations indicate that PDPN-SCs are a heterogeneous cell population and suggest that OSX-positive PDPN-SCs contribute to bone formation.

Periarteriolar PDPN-SCs emerge in a de novo fashion on the diaphyseal arteriole

We investigated the PDPN-SCs in the diaphyseal marrow, cortical bone, and metaphysis; however, PDPN-SCs in the vicinity of diaphyseal arterioles remain to be examined. Periarteriolar PDPN-SCs were detected at 3 w.o but not at 2 w.o of age (Fig. 1). To examine when and how PDPN-SCs appear in the perivascular region, we observed femurs in 1.5–3.0 w.o of age (Fig. 5). In 1.5 w.o femur, although diaphyseal arterioles were not surrounded by PDPN-SCs, we observed that a single cell of PDPN-SC resided on the arteriole (Fig. 5A). Further observations showed that a part of diaphyseal arterioles began to be surrounded by PDPN-SCs in 2.0 w.o femur (Fig. 5B). In addition, periarteriolar PDPN-SCs tended to appear predominantly on arterioles adjacent to the central vein. In 3.0 w.o femur, the diaphyseal arterioles were entirely ensheathed by PDPN-SCs, after which PDPN-SCs continued to be present around the diaphyseal arterioles as perivascular cells (Fig. 5C and D). These observations suggested that periarteriolar PDPN-SCs emerged *de novo* on the diaphyseal arteriole and populated the area as perivascular cells.

Discussion

In the present study, we examined the spatiotemporal transition of PDPN-SCs in the postnatal femur (Fig. 6). PDPN-SCs were present within the POC-related femoral regions: the primitive diaphyseal marrow, cortical bone, and metaphysis in neonates. The localized distribution of PDPN-SCs altered in association with tissue growth. In the cortical bone, PDPN-SCs were present in the periosteum and part of the endosteum. In the metaphysis, PDPN-SCs were located on the trabecular bones. In the diaphysis, PDPN-SCs in the primary marrow disappeared with tissue growth, whereas peri-arteriolar PDPN-SCs emerged *de novo*. Additionally, PDPN-SCs were divided into two subsets: OSX-positive and -negative cells.

A subset of bone marrow-MSPCs that expresses OSX is committed to the osteolineage and stromal cells in the neonatal stage, which contributes to femoral osteogenesis and regeneration of injured bone [32]. Perinatally labeled OSX-expressing MSPCs are abundant in the cortical and trabecular bones of the metaphysis and disappear with ontogenetic growth. This spatiotemporal behavior of the OSX-expressing MSPCs is comparable to those of the PDPN-SCs we observed. These insights suggest that OSX-positive PDPN-SCs are a subset of OSX-expressing MSPCs that contribute to the formation of bone parenchyma. We also detected OSX-negative PDPN-SCs in the femur. In the cortical bone, OSX-negative PDPN-SCs tended to be present in the periosteum and endosteum. The periosteum and endosteum include tissue-resident stem and progenitor cells such as skeletal

stem/progenitor cells (SSC/SSPC) [19-22, 33]. In addition, we previously reported that one population of primary SSCs/SSPCs expressed PDPN in mice [26]. Based on the literature, we consider that OSX-negative PDPN-SCs are undifferentiated progenitor cells of the SSC lineage. OSX-negative PDPN-SCs in the metaphysis are also presumed to be SSC-lineage progenitor cells, similar to those in the peri/endosteum.

In previous studies [26, 27, 29] and the present study, we have investigated the role and behavior of PDPN-SCs in the bone and marrow. However, this study has several limitations. Herein, we demonstrate that periarteriolar PDPN-SCs appear sporadically, although the cellular origin of periarteriolar PDPN-SCs remains unclear. Previous reports have revealed that several stromal progenitor cells, such as Nestin^{GFP}/NG2-positive cells, populate the periarteriolar region and constitute the hematopoietic microenvironment [12, 16, 34]. We speculate that periarteriolar PDPN-SCs are generated from these stromal progenitor cells. In addition, the spatiotemporal behavior of periarteriolar PDPN-SCs raises another scientific question: why do PDPN-SCs need to emerge on the arterioles late in marrow vascular network development? Given the physiological roles of periarteriolar PDPN-SCs in promoting megakaryo/erythropoiesis [27, 29], we hypothesize that PDPN-SCs are involved in tissue-environmental remodeling of the diaphyseal marrow, from neonatal/postnatal conditions to adult conditions. To elucidate the mechanism underlying the *de novo* appearance and physiological roles of periarteriolar PDPN-SCs, *in situ* gene expression analyses, such as

spatial transcriptome analysis, are necessary. An *in vivo* cell fate reporter or depletion model must also be established. Furthermore, a spatiotemporal analysis during the embryonic stage could help us understand the cellular origin and function of PDPN-SCs in POC-related portions of the femur.

This study shows the spatiotemporal distribution and transition of PDPN-SCs within POC-related femoral regions. The identification of the OSX-positive PDPN-SC subset raises the possibility that PDPN-SCs contribute to bone formation. This study provides a new perspective on the involvement of stromal cells in postnatal bone and marrow formation. Further studies will provide insights into the biological nature of bone marrow stromal cells and the mechanisms of tissue growth, remodeling, and regeneration in the bone and bone marrow.

Acknowledgements

We would like to thank Editage (www.editage.jp) for English language editing.

Data availability statement

Data generated in this study are available from the corresponding author upon reasonable request.

Author contributions

H.N., R. N., N. T., and S. T. methodology; H.N., R. N., and S. T., investigation; H. N., R. N., Nobuaki. S., A. S., S. O., and S. T. formal analysis; H. N and S.T. writing–original draft; Nobuaki S., A. S., S. O., T. Kanematsu., Naruko S. A. K., T. Kojima, K. S-I., T. M., and S. T. supervision; Nobuaki S., T. Kojima, T. M., and S. T. conceptualization; H. N., R. N., Nobuaki S., A. S., S. O., T. Kanematsu., Naruko S. A. K., T. Kojima, T. M., and S. T. writing–review and editing; H. N., S. Y., Nobuaki S., A. S., S. O., T. Kanematsu., Naruko S. A. K., T. Kojima, T. M., and S. T. data curation; Nobuaki S., A. K., T. Kojima, T. M., and S. T. funding acquisition; S. T. validation; S. T. visualization; S. T. project administration.

Funding

This study was supported by grants-in-aid provided by the Japanese Ministry of Education,

Culture, Sports, Science, and Technology (Grant No. 22K06881 to S. T. and Grant No. 22K08518 to A. K.), the National Center for Geriatrics and Gerontology (NCGG, the Research Funding for Longevity Sciences, Grant No. 22-10 to A. K.), the Takeda Science Foundation (to S. T.), the SENSHIN Medical Research Foundation (to S. T.), SUHARA Memorial Foundation (to S. T.), and JST FOREST Program (Grant No. JPMJFR2158 to S. T.).

Declaration of competing interest

The authors declare that they have no conflicts of interest regarding the content of this article.

Figure legends

Figure 1. Distribution of PDPN-expressing stromal cells (PDPN-SCs) in the postnatal mouse femur.

A. Schematic of the femur. B–M. Representative IHC images of the postnatal femur from postnatal day 0, shown as 0 weeks old (0 w.o) to three weeks old (3 w.o.). The left panels (B, E, H, and K) are IHC images of the longitudinal section. The middle panels (C, F, I, and L) are high-magnification images focusing on the metaphysis of the left panel. The right panels (D, G, J, and M) are IHC images of the transverse section. Cryosections were stained with PDPN (green), CD31 (red), and DAPI (white). Scale bars in the left panels indicate 1000 μm. Scale bars in the middle and right panels indicate 100 μm. DAPI, 40,6-diamidino-2-phenylindole; IHC, immunohistochemistry; PDPN, podoplanin.

Figure 2. Quantitative analysis of PDPN-SCs in the diaphyseal marrow, cortical bone, and metaphysis during postnatal age progression.

A. Representative longitudinal IHC images of the diaphyseal marrow in the femur at 0–2 w.o. B. Quantitative data of PDPN-SCs in the diaphyseal marrow at 0–2 w.o. C. Representative longitudinal IHC images of the cortical bone in the femur at 0–2 w.o. D. Quantitative data of PDPN-SCs in the cortical bone at 0–2 w.o. The number of PDPN-SCs in the cortical bone was evaluated from the transverse IHC images of the femur. E. Representative longitudinal IHC

images of the metaphysis in the femur at 0–2 w.o. F. Quantitative data of PDPN-SCs in the metaphysis at 0–2 w.o. Cryosections were stained with PDPN (green), CD31 (red), and DAPI (white). Scale bars in the middle and right panels indicate 100 μm. DAPI, 4′,6-diamidino-2-phenylindole; IHC, immunohistochemistry; PDPN, podoplanin. *$p < 0.05$. **$p < 0.01$. Statistical analysis was performed using one-way ANOVA and Tukey's multiple comparison test (n = 3 per group). The error bars represent SDs.

Figure 3. Tissue growth associated transition of PDPN-SCs in the diaphyseal marrow, cortical bone, and metaphysis.

A. Quantitative data of the CD31-positive area in the diaphyseal marrow. The CD31-positive area was calculated as a percentage of the total marrow area. B. Correlation between the number of PDPN-SCs and the CD31-positive area in the diaphyseal marrow. C. Quantitative data of the CD31-positive area in the cortical bone. The CD31-positive area was calculated as a percentage of the total cortical bone area. D. Correlation between the number of PDPN-SCs and the CD31-positive area in the cortical bone. E. Area index of the metaphysis. The area index was calculated by the area of the metaphysis and the diaphysis, which assesses the metaphysis growth with age progression. F. Correlation between the number of PDPN-SCs and the area index of the metaphysis. *$p < 0.05$. **$p < 0.01$. ***$p < 0.001$. ****$p < 0.0001$. Statistical analysis was performed using one-way ANOVA and Tukey's multiple comparison

test (n = 3 per group). Error bars represent SDs.

Figure 4. A novel subset, OSX-positive PDPN-SC, is present in the diaphyseal marrow, cortical bone, and metaphysis.

A. Representative IHC images of diaphyseal marrow in the 0 and 1 w.o femoral longitudinal sections. B. Representative IHC images of cortical bone in the 0–3 w.o femoral longitudinal sections. C. Representative IHC images of metaphysis in the 0–3 w.o femoral longitudinal sections. The filled and open arrowheads indicate OSX-positive and OSX-negative PDPN-SCs, respectively. Cryosections were stained with PDPN (green), OSX (red), and DAPI (white). Scale bars indicate 50 μm. DAPI, 4′,6-diamidino-2-phenylindole; IHC, immunohistochemistry; PDPN, podoplanin; OSX, osterix, periosteum; PO, trabecular bone; TB.

Figure 5. *De novo* emerged PDPN-SCs ensheathe diaphyseal marrow arterioles.

A. Representative longitudinal IHC image of the diaphyseal marrow arteriole in the 1.5 w.o. femur. The arrowhead indicates *de novo* emerged single cell PDPN-SC. B. Representative longitudinal IHC image of the diaphyseal marrow arterioles in 2 w.o femur. Panels B-i and B-ii show the arteriole without PDPN-SCs. Panel B-iii represents the arteriole surrounded by PDPN-SCs. The arrowhead indicates PDPN-SC ensheathing the arteriole. C. Representative

longitudinal IHC image of the diaphyseal marrow arterioles in the 3 w.o. femur. CV indicates central vein. D. Representative transverse IHC images of the diaphyseal marrow arteriole in 4, 6, and 8 w.o femurs. Cryosections were stained with PDPN (green), CD31 (red), and DAPI (white). The scale bar in the A-left indicates 100 μm. Scale bars in A-middle and right indicate 25 μm. The scale bar in the B-upper panel indicates 1000 μm. The scale bars in B lower panels indicate 50 μm. Scale bars in C indicate 100 μm. Scale bars in D indicate 20 μm. DAPI, 4′,6-diamidino-2-phenylindole; IHC, immunohistochemistry; PDPN, podoplanin; OSX, osterix.

Figure 6. Graphical summary depicting the spatiotemporal behavior of PDPN-SCs in the postnatal femur.

A. Schematic picture of longitudinal mouse femur of 0 w.o. Green layers indicate PDPN-SC-positive regions. Red lines indicate blood vessels. A. Schematic picture of longitudinal mouse femur of >2 w.o. Green layers indicate PDPN-SC-positive regions. Red lines indicate blood vessels. Three types of vasculatures, central vein, arteriole, and sinusoid are annotated. C. Tissue-growth associated time transition of PDPN-SCs in the cortical bone. PDPN-SCs are abundantly present in the primitive bone and periosteum. After tissue growth, PDPN-SCs are restrictedly present in the periosteum and a part of the endosteum. D. Tissue-growth associated time transition of PDPN-SCs in the metaphysis. PDPN-SCs are present in the

primary region of the neonatal metaphysis. After tissue growth, PDPN-SCs reside on the trabecular bones. E. Tissue growth associated time transition of PDPN-SCs on the diaphyseal arteriole. Periarteriolar PDPN-SCs appear sporadically between 1–2 w.o and populate to surround the arterioles. C–E. PDPN-SCs are shown as green cytoplasmic cells. Red lines indicate blood vessels.

References

[1] Kronenberg HM. Developmental regulation of the growth plate. *Nature.* 2003;423(6937):332–6.

[2] Karsenty G, Wagner EF. Reaching a genetic and molecular understanding of skeletal development. *Dev Cell.* 2002;2(4):389–406.

[3] Maes C, Kobayashi T, Selig MK, Torrekens S, Roth SI, Mackem S, Carmeliet G, Kronenberg HM. Osteoblast precursors, but not mature osteoblasts, move into developing and fractured bones along with invading blood vessels. *Dev Cell.* 2010;19(2):329–44.

[4] Matsushita Y, Chu AKY, Tsutsumi-Arai C, Orikasa S, Nagata M, Wong SY, Welch JD, Ono W, Ono N. The fate of early perichondrial cells in developing bones. *Nat Commun.* 2022;13(1):7319.

[5] Maes C, Kobayashi T, Kronenberg HM. A novel transgenic mouse model to study the osteoblast lineage in vivo. *Ann N Y Acad Sci.* 2007;1116:149–64.

[6] Ding DC, Shyu WC, Lin SZ. Mesenchymal stem cells. *Cell Transplant.* 2011;20(1):5–14.

[7] Matsushita Y, Nagata M, Kozloff KM, Welch JD, Mizuhashi K, Tokavanich N, Hallett SA, Link DC, Nagasawa T, Ono W, Ono N. A Wnt-mediated transformation of the bone marrow stromal cell identity orchestrates skeletal regeneration. *Nat Commun*. 2020;11(1):332.

[8] Yue R, Zhou BO, Shimada IS, Zhao Z, Morrison SJ. Leptin Receptor Promotes Adipogenesis and Reduces Osteogenesis by Regulating Mesenchymal Stromal Cells in Adult

Bone Marrow. *Cell Stem Cell*. 2016;18(6):782–96.

[9] Worthley DL, Churchill M, Compton JT, Tailor Y, Rao M, Si Y, Levin D, Schwartz MG, Uygur A, Hayakawa Y, Gross S, Renz BW, Setlik W, Martinez AN, Chen X, Nizami S, Lee HG, Kang HP, Caldwell JM, Asfaha S, Westphalen CB, Graham T, Jin G, Nagar K, Wang H, Kheirbek MA, Kolhe A, Carpenter J, Glaire M, Nair A, Renders S, Manieri N, Muthupalani S, Fox JG, Reichert M, Giraud AS, Schwabe RF, Pradere JP, Walton K, Prakash A, Gumucio D, Rustgi AK, Stappenbeck TS, Friedman RA, Gershon MD, Sims P, Grikscheit T, Lee FY, Karsenty G, Mukherjee S, Wang TC. Gremlin 1 identifies a skeletal stem cell with bone, cartilage, and reticular stromal potential. *Cell*. 2015;160(1–2):269–84.

[10] Zhou BO, Yue R, Murphy MM, Peyer JG, Morrison SJ. Leptin-receptor-expressing mesenchymal stromal cells represent the main source of bone formed by adult bone marrow. *Cell Stem Cell*. 2014;15(2):154–68.

[11] Omatsu Y, Seike M, Sugiyama T, Kume T, Nagasawa T. Foxc1 is a critical regulator of haematopoietic stem/progenitor cell niche formation. *Nature*. 2014;508(7497):536–40.

[12] Kunisaki Y, Bruns I, Scheiermann C, Ahmed J, Pinho S, Zhang D, Mizoguchi T, Wei Q, Lucas D, Ito K, Mar JC, Bergman A, Frenette PS. Arteriolar niches maintain haematopoietic stem cell quiescence. *Nature*. 2013;502(7473):637–43.

[13] Park D, Spencer JA, Koh BI, Kobayashi T, Fujisaki J, Clemens TL, Lin CP, Kronenberg HM, Scadden DT.Endogenous bone marrow MSCs are dynamic, fate-restricted participants in

bone maintenance and regeneration. *Cell Stem Cell*. 2012;10(3):259–72.

[14] Ding L, Saunders TL, Enikolopov G, Morrison SJ. Endothelial and perivascular cells maintain haematopoietic stem cells. *Nature*. 2012;481(7382):457–62.

[15] Omatsu Y, Sugiyama T, Kohara H, Kondoh G, Fujii N, Kohno K, Nagasawa T. The essential functions of adipo-osteogenic progenitors as the hematopoietic stem and progenitor cell niche. *Immunity*. 2010;33(3):387–99.

[16] Méndez-Ferrer S, Michurina TV, Ferraro F, Mazloom AR, Macarthur BD, Lira SA, Scadden DT, Ma'ayan A, Enikolopov GN, Frenette PS. Mesenchymal and haematopoietic stem cells form a unique bone marrow niche. *Nature*. 2010;466(7308):829–34.

[17] Sugiyama T, Kohara H, Noda M, Nagasawa T. Maintenance of the hematopoietic stem cell pool by CXCL12-CXCR4 chemokine signaling in bone marrow stromal cell niches. *Immunity*. 2006;25(6):977–88.

[18] Ara T, Tokoyoda K, Sugiyama T, Egawa T, Kawabata K, Nagasawa T. Long-term hematopoietic stem cells require stromal cell-derived factor-1 for colonizing bone marrow during ontogeny. *Immunity*. 2003;19(2):257–67.

[19] Tournaire G, Stegen S, Giacomini G, Stockmans I, Moermans K, Carmeliet G, van Gastel N. Nestin-GFP transgene labels skeletal progenitors in the periosteum. *Bone*. 2020;133:115259.

[20] Ortinau LC, Wang H, Lei K, Deveza L, Jeong Y, Hara Y, Grafe I, Rosenfeld SB, Lee D,

Lee B, Scadden DT, Park D. Identification of Functionally Distinct Mx1+alphaSMA+ Periosteal Skeletal Stem Cells. *Cell Stem Cell*. 2019;25(6):784–796 e5.

[21] Duchamp de Lageneste O, Julien A, Abou-Khalil R, Frangi G, Carvalho C, Cagnard N, Cordier C, Conway SJ, Colnot C. Periosteum contains skeletal stem cells with high bone regenerative potential controlled by Periostin. *Nat Commun*. 2018;9(1):773.

[22] Deveza L, Ortinau L, Lei K, Park D: Comparative analysis of gene expression identifies distinct molecular signatures of bone marrow- and periosteal-skeletal stem/progenitor cells. *PLoS One*. 2018;13(1):e0190909.

[23] Mizuhashi K, Ono W, Matsushita Y, Sakagami N, Takahashi A, Saunders TL, Nagasawa T, Kronenberg HM, Ono N. Resting zone of the growth plate houses a unique class of skeletal stem cells. *Nature*. 2018;563(7730):254–258.

[24] Chan CK, Seo EY, Chen JY, Lo D, McArdle A, Sinha R, Tevlin R, Seita J, Vincent-Tompkins J, Wearda T, Lu WJ, Senarath-Yapa K, Chung MT, Marecic O, Tran M, Yan KS, Upton R, Walmsley GG, Lee AS, Sahoo D, Kuo CJ, Weissman IL, Longaker MT. Identification and specification of the mouse skeletal stem cell. *Cell*. 2015;160(1–2):285–98.

[25] Shen F, Huang X, He G, Shi Y. The emerging studies on mesenchymal progenitors in the long bone, Cell Biosci 2023;13(1):105.

[26] Tamura S, Mukaide M, Katsuragi Y, Fujii W, Odaira K, Suzuki N, Tsukiji N, Okamoto S, Suzuki A, Kanematsu T, Katsumi A, Takagi A, Ikeda K, Ueyama J, Hirayama M, Suzuki-

Inoue K, Matsushita T, Kojima T, Hayakawa F. Periosteum-derived podoplanin-expressing stromal cells regulate nascent vascularization during epiphyseal marrow development, *J Biol Chem*. 2022;298(5):101833.

[27] Tamura S, Suzuki-Inoue K, Tsukiji N, Shirai T, Sasaki T, Osada M, Satoh K, Ozaki Y. Podoplanin-positive periarteriolar stromal cells promote megakaryocyte growth and proplatelet formation in mice by CLEC-2. *Blood*. 2016;127(13):1701–10.

[28] Baccin C, Al-Sabah J, Velten L, Helbling PM, Grünschläger F, Hernández-Malmierca P, Nombela-Arrieta C, Steinmetz LM, Trumpp A, Haas S. Combined single-cell and spatial transcriptomics reveal the molecular, cellular and spatial bone marrow niche organization. *Nat Cell Biol*. 2020;22(1):38–48.

[29] Otake S, Sasaki T, Shirai T, Tsukiji N, Tamura S, Takano K, Ozaki Y, Suzuki-Inoue K. CLEC-2 stimulates IGF-1 secretion from podoplanin-positive stromal cells and positively regulates erythropoiesis in mice. *J Thromb Haemost*. 2021;19(6):1572–1584.

[30] Hooper AT, Butler JM, Nolan DJ, Kranz A, Iida K, Kobayashi M, Kopp HG, Shido K, Petit I, Yanger K, James D, Witte L, Zhu Z, Wu Y, Pytowski B, Rosenwaks Z, Mittal V, Sato TN, Rafii S. Engraftment and reconstitution of hematopoiesis is dependent on VEGFR2-mediated regeneration of sinusoidal endothelial cells. *Cell Stem Cell*. 2009;4(3):263–74.

[31] Ramasamy SK. Structure and Functions of Blood Vessels and Vascular Niches in Bone. *Stem Cells Int*. 2017;2017:5046953.

[32] Mizoguchi T, Pinho S, Ahmed J, Kunisaki Y, Hanoun M, Mendelson A, Ono N, Kronenberg HM, Frenette PS. Osterix marks distinct waves of primitive and definitive stromal progenitors during bone marrow development. *Dev Cell*. 2014;29(3):340–9.

[33] Matsushita Y, Liu J, Chu AKY, Tsutsumi-Arai C, Nagata M, Arai Y, Ono W, Yamamoto K, Saunders TL, Welch JD, Ono N. Bone marrow endosteal stem cells dictate active osteogenesis and aggressive tumorigenesis. *Nat Commun*. 2023;14(1):2383.

[34] Asada N, Kunisaki Y, Pierce H, Wang Z, Fernandez NF, Birbrair A, Ma'ayan A, Frenette PS. Differential cytokine contributions of perivascular haematopoietic stem cell niches. *Nat Cell Biol*. 2017;19(3):214–223.

Figure.1

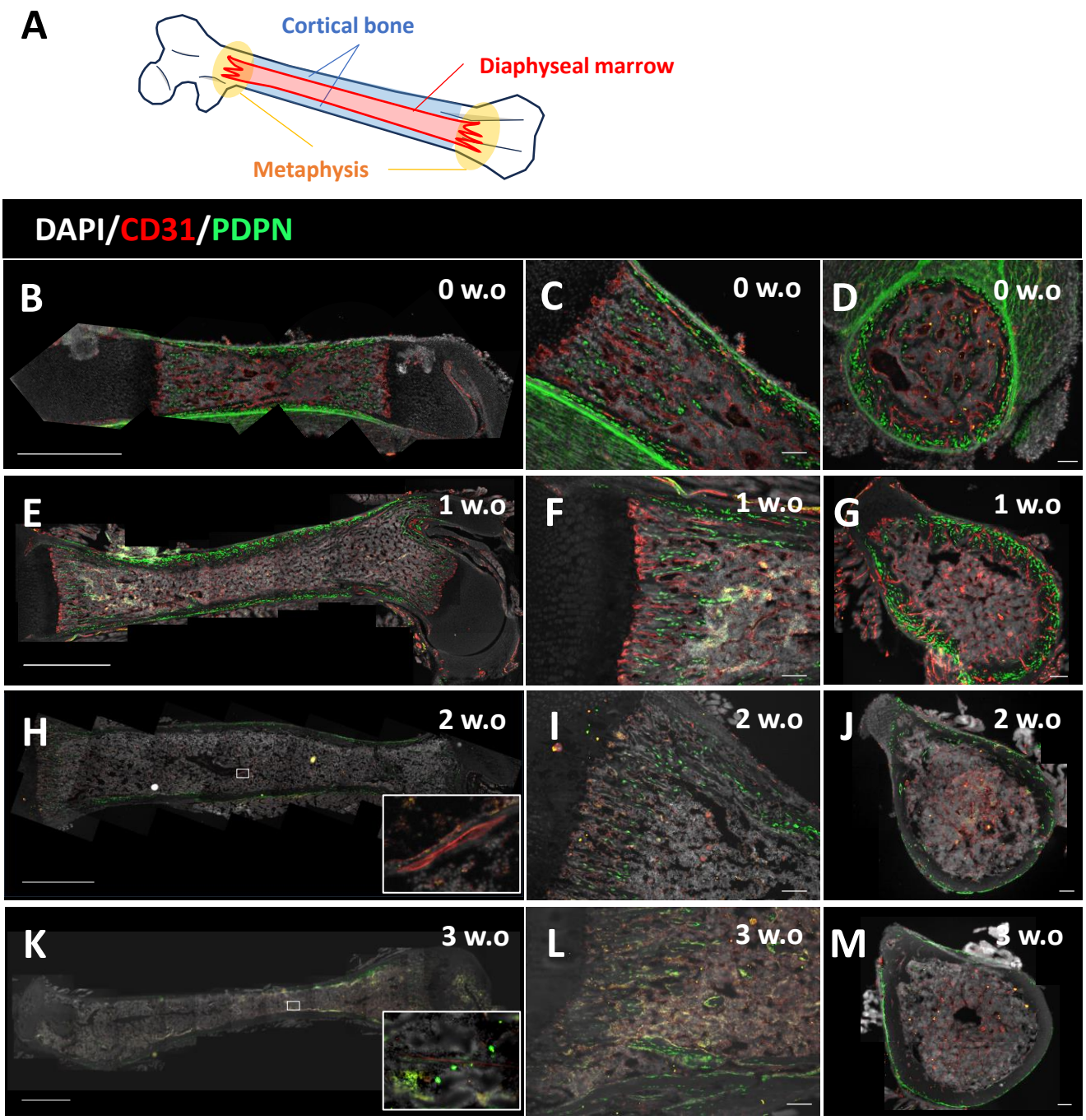
A
Cortical bone
Diaphyseal marrow
Metaphysis
DAPI/CD31/PDPN
B
0 w.o
C
0 w.o
D
0 w.o
E
1 w.o
F
1 w.o
G
1 w.o
H
2 w.o
I
2 w.o
J
2 w.o
K
3 w.o
L
3 w.o
M
3 w.o

Figure.2

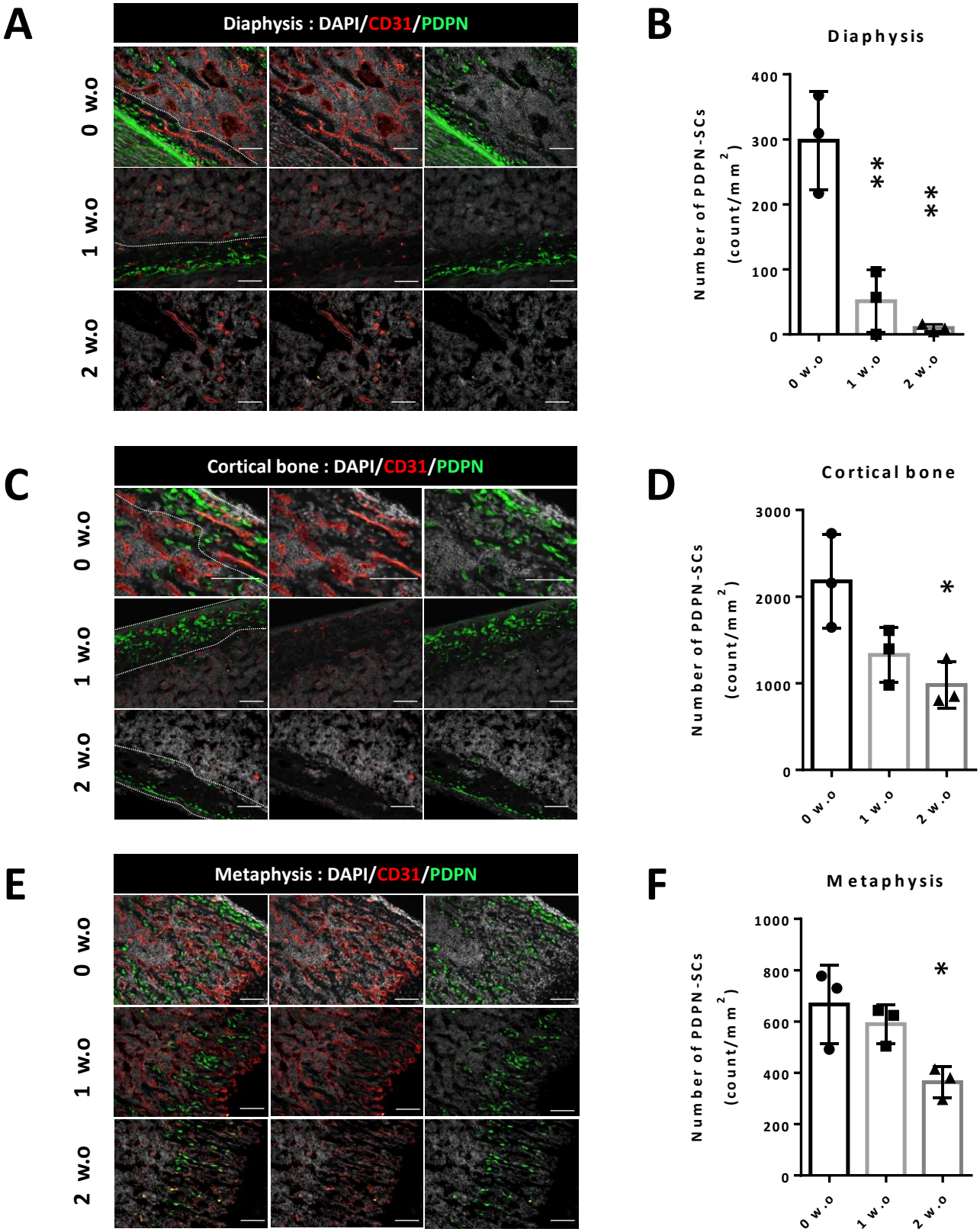
A
Diaphysis : DAPI/CD31/PDPN
0 w.o
1 w.o
2 w.o
B
Diaphysis
Number of PDPN-SCs (count/mm2)
400
300
200
100
0
0 w.o
1 w.o
2 w.o
C
Cortical bone : DAPI/CD31/PDPN
0 w.o
1 w.o
2 w.o
D
Cortical bone
Number of PDPN-SCs (count/mm2)
3000
2000
1000
0
0 w.o
1 w.o
2 w.o
E
Metaphysis : DAPI/CD31/PDPN
0 w.o
1 w.o
2 w.o
F
Metaphysis
Number of PDPN-SCs (count/mm2)
1000
800
600
400
200
0
0 w.o
1 w.o
2 w.o

Figure.3

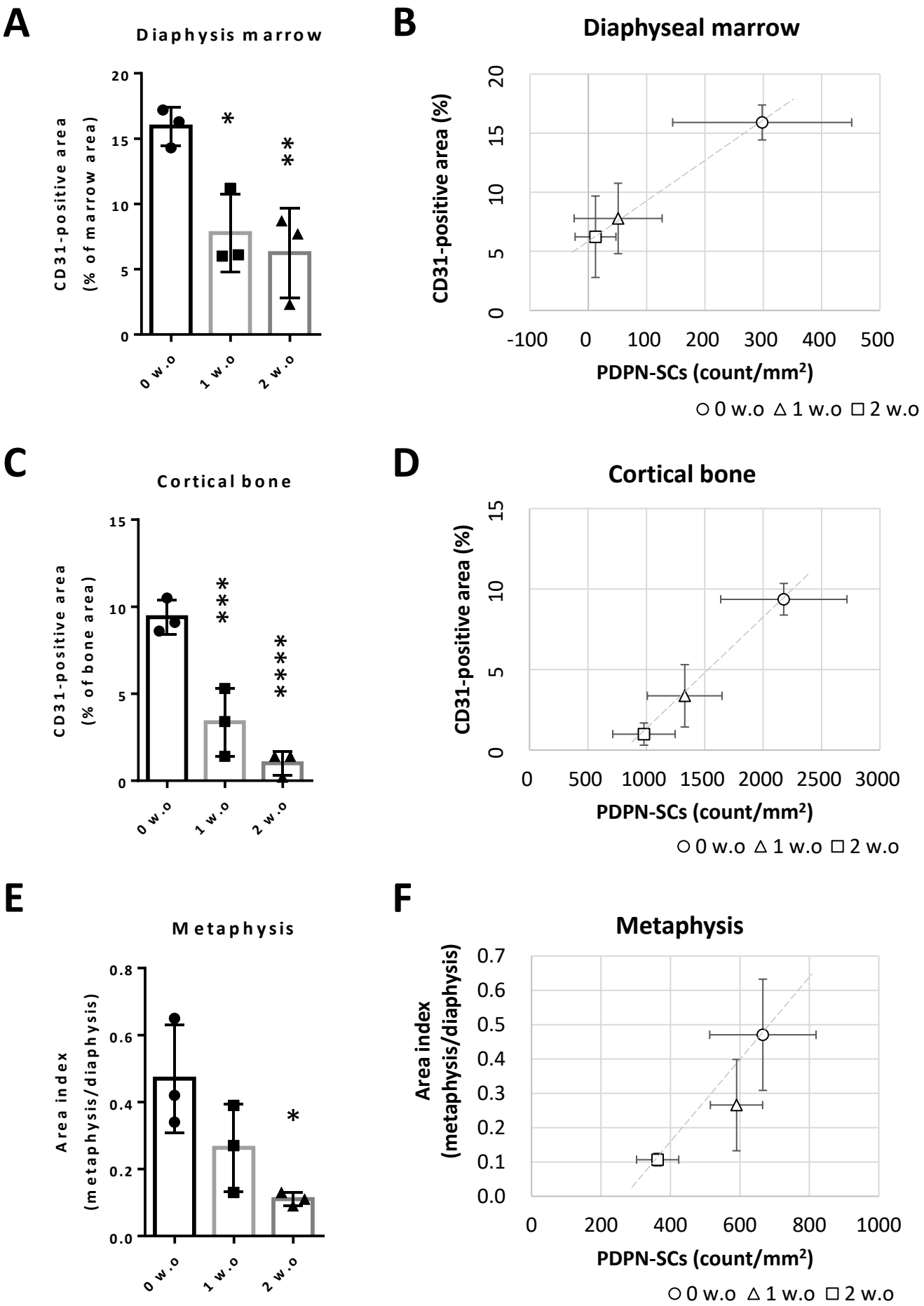
A
Diaphysis marrow
CD31-positive area
(% of marrow area)
20
15
10
5
0
*
**
0 w.o
1 w.o
2 w.o
B
Diaphyseal marrow
CD31-positive area (%)
20
15
10
5
0
-100
0
100
200
300
400
500
PDPN-SCs (count/mm²)
○ 0 w.o △ 1 w.o □ 2 w.o
C
Cortical bone
CD31-positive area
(% of bone area)
15
10
5
0
***
****
0 w.o
1 w.o
2 w.o
D
Cortical bone
CD31-positive area (%)
15
10
5
0
0
500
1000
1500
2000
2500
3000
PDPN-SCs (count/mm²)
○ 0 w.o △ 1 w.o □ 2 w.o
E
Metaphysis
Area index
(metaphysis/diaphysis)
0.8
0.6
0.4
0.2
0.0
*
0 w.o
1 w.o
2 w.o
F
Metaphysis
Area index
(metaphysis/diaphysis)
0.7
0.6
0.5
0.4
0.3
0.2
0.1
0.0
0
200
400
600
800
1000
PDPN-SCs (count/mm²)
○ 0 w.o △ 1 w.o □ 2 w.o

Figure.4

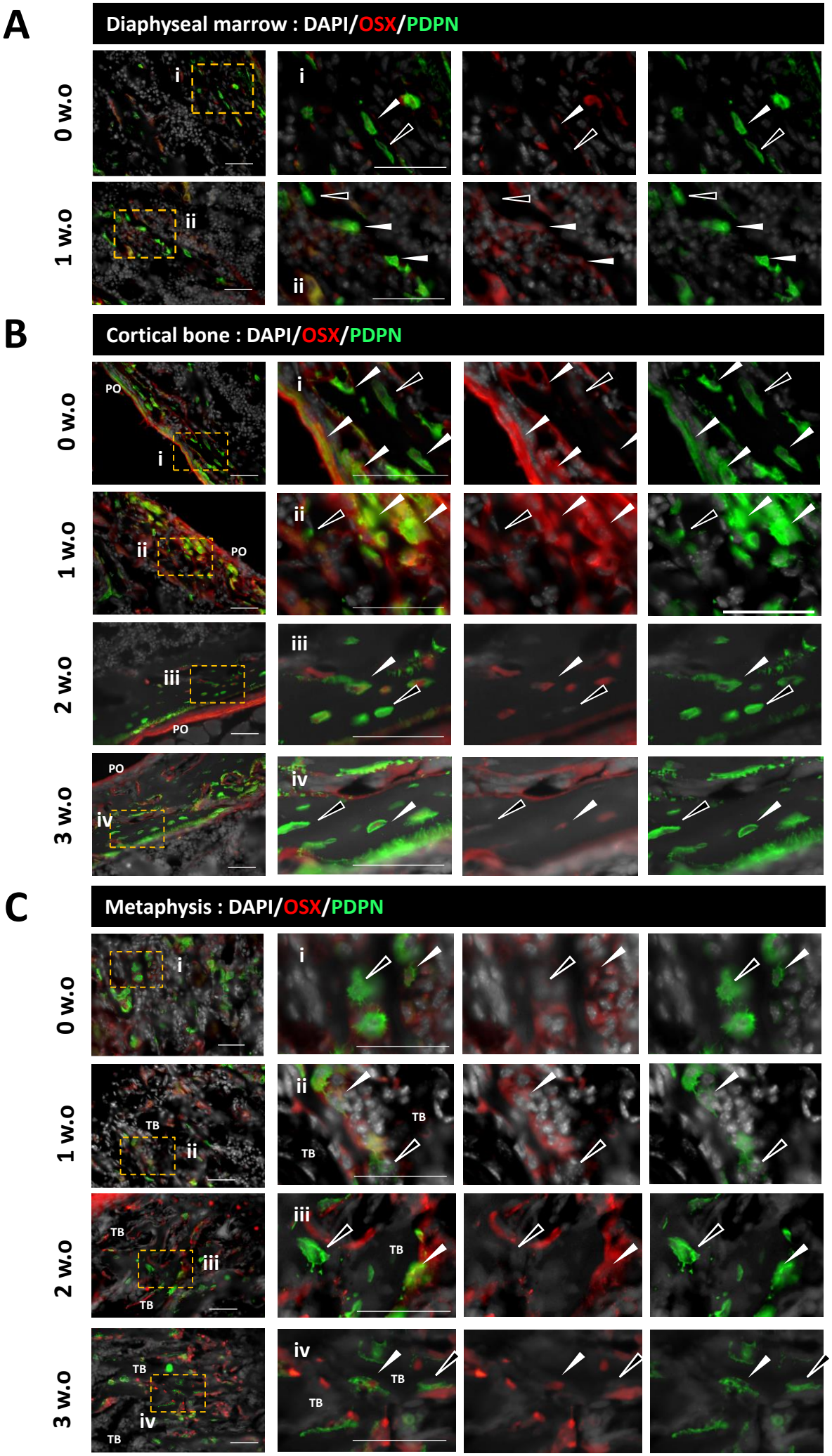
A
Diaphyseal marrow : DAPI/OSX/PDPN
0 w.o
1 w.o
i
ii
B
Cortical bone : DAPI/OSX/PDPN
0 w.o
1 w.o
2 w.o
3 w.o
PO
i
ii
iii
iv
C
Metaphysis : DAPI/OSX/PDPN
0 w.o
1 w.o
2 w.o
3 w.o
TB
i
ii
iii
iv

Figure.5

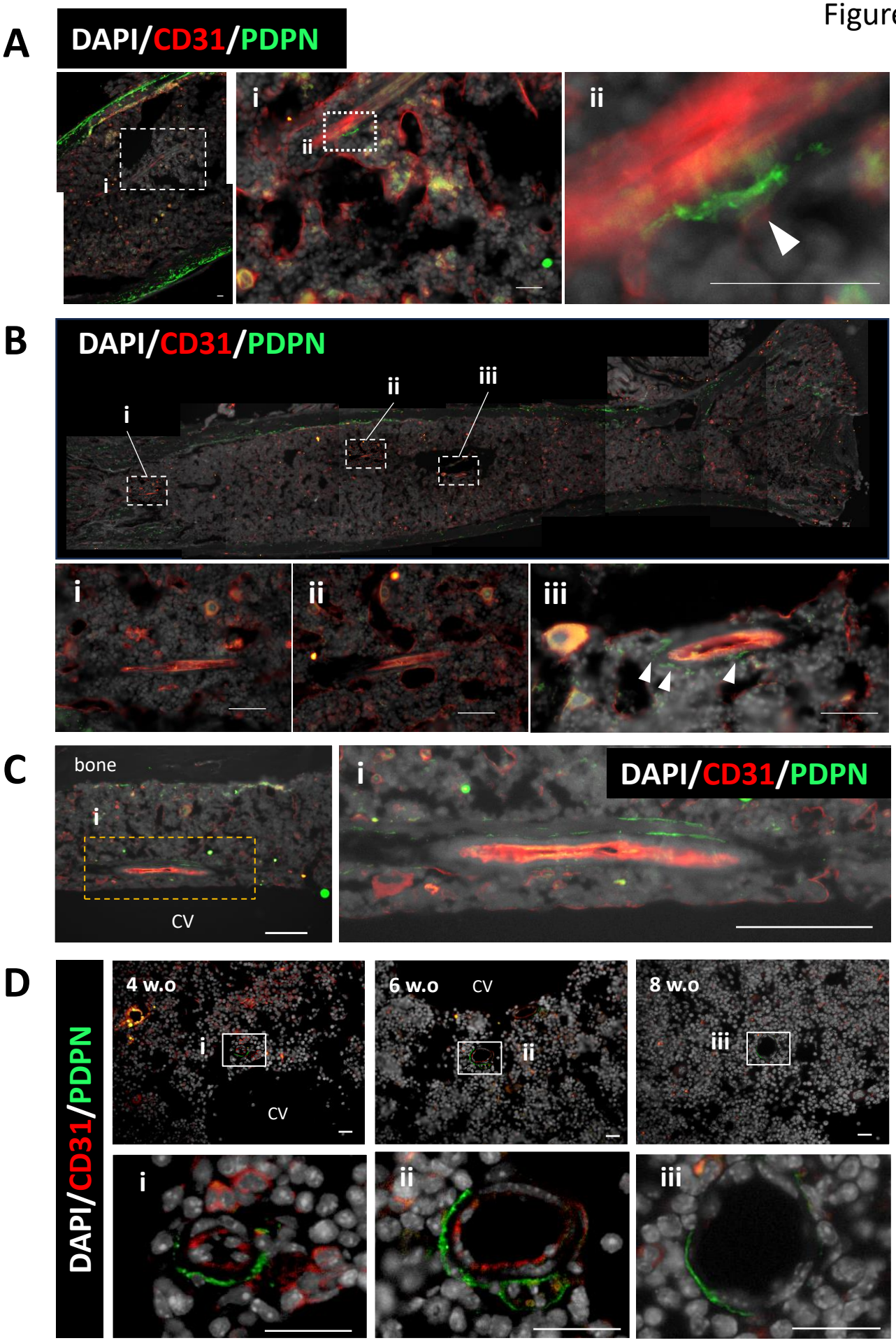
A
DAPI/CD31/PDPN
i
ii
B
DAPI/CD31/PDPN
i
ii
iii
C
bone
i
CV
DAPI/CD31/PDPN
D
DAPI/CD31/PDPN
4 w.o
6 w.o
8 w.o
CV

Figure.6

A **0 w.o.**

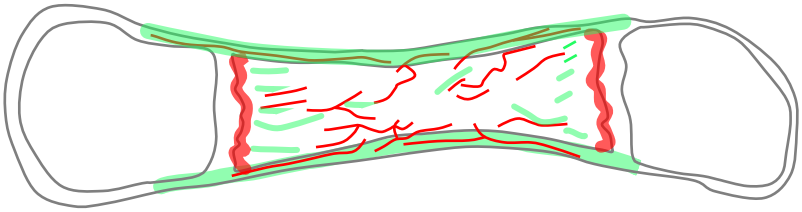

B **2 w.o. ~**

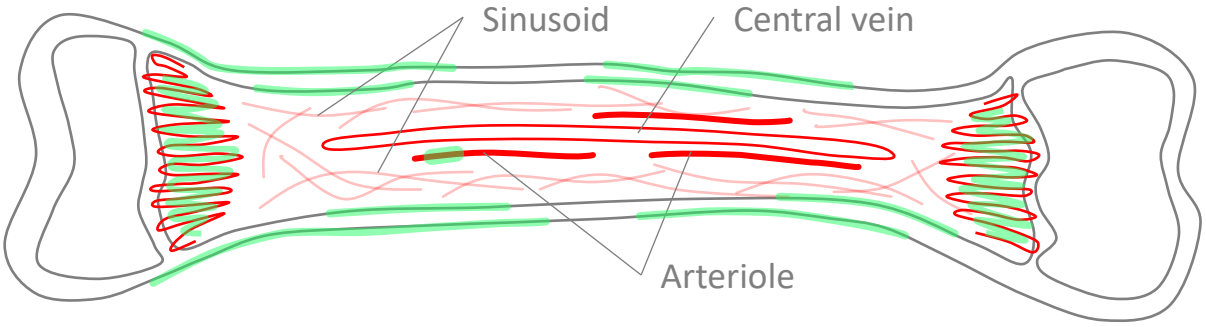

C **Cortical bone**

~ 1 w.o. **2 w.o. ~**

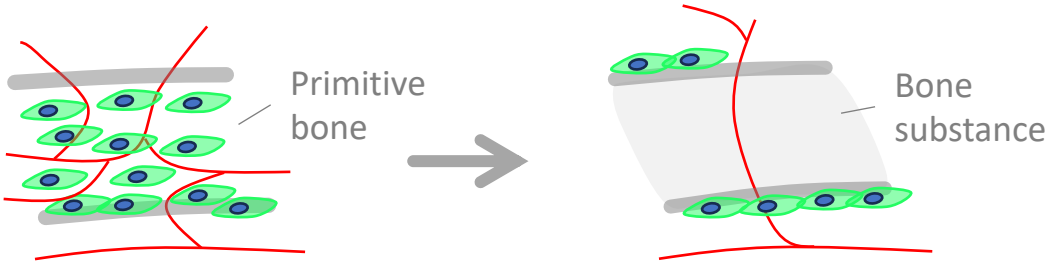

D **Metaphysis**

~ 1 w.o. **2 w.o. ~**

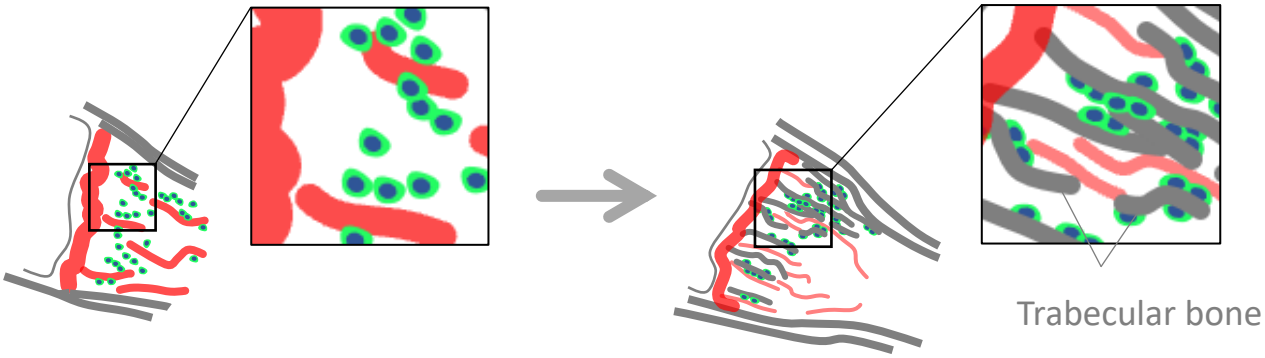

E **Diaphyseal arteriole**
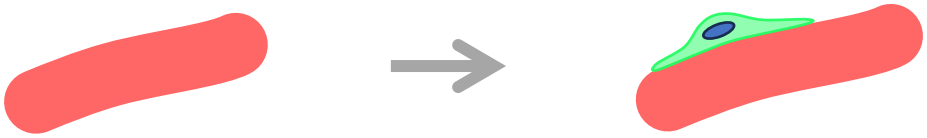
~ 1 w.o. **2 w.o. ~**